Appl Phys A (2010) 99: 921–929
DOI 10.1007/s00339-010-5681-5

Applied Physics A
Materials Science & Processing

Electrochromic properties of nanocrystalline WO_3 thin films grown on flexible substrates by plasma-assisted evaporation technique

K. Hari Krishna · O.M. Hussain · C.M. Julien

Received: 1 October 2009 / Accepted: 10 March 2010 / Published online: 15 April 2010

Abstract Thin films of Tungsten trioxide (WO_3) were deposited on ITO-coated flexible Kapton substrates by plasma-assisted activated reactive evaporation (ARE) technique. The influence of growth and microstructure on optoelectrochromic properties of WO_3 thin films was studied. The nanocrystalline WO_3 films grown at substrate temperature of 250°C were composed of vertically elongated cone-shaped grains of size 65 nm with relative density of 0.71. These WO_3 films demonstrated higher optical transmittance of 85% in the visible region with estimated optical band gap of 3.39 eV and exhibited better optical modulation of 66% and coloration efficiency of 52.8 cm^2/C at the wavelength of 550 nm.

1 Introduction

Electrochromism (EC) is one of the growing technologies in which physics, chemistry, materials science, and engineering are greatly involved in revealing the in-depth mechanism of coloring and bleaching [1, 2]. This EC technology has attracted by attention of researchers due to its unique characteristic of optical transmittance transfer, which provides some potential applications, such as architectural "smart windows", nonemissive displays, variable-reflectance mirrors, variable-transmittance eye wear for a variety of applications, and variable-emittance surfaces for temperature stabilization of space vehicles [3–5]. Among several electrochromic materials, tungsten trioxide (WO_3) has long been recognized as one of the potential cathodic electrochromic material owing its exceptional electrochromic properties, like coloration efficiency, reversibility, stability, good response time, and high capacity for inserted ions [6–8]. The WO_3 thin films have attracted much attention due to their superior characteristics of low power consumption and low stress for viewer's eyes [9]. In these films, electrochromic property is achieved by the insertion of Li^+ ions into WO_3 thin film as a result the valance state of W^{6+} changes to a W^{6+}/W^{5+} mixed state [10]. It is noteworthy that the EC properties of WO_3 thin films strongly depend on physical and chemical properties of the films, which in turn depend upon thin film deposition technique and respective film processing parameters. Various physical and chemical vapor thin film deposition techniques, such as pulsed laser deposition [11], sputtering [12], electron-beam evaporation technique [13], thermal evaporation [14], sol–gel [15], spin coating [16] techniques, have been employed to prepare WO_3 thin films.

Activated reactive evaporation technique (ARE) is one of the plasma assisted thin film deposition techniques to prepare thin films with high deposition rates at relatively low substrate temperature and widely accepted for the growth of refractory compounds and their related materials. In the activated reactive evaporation, the reaction occurs predominantly in plasma and chemical composition of the films can be controlled by changing the ratio of reacting species. In addition to the chemical composition, the grain size and surface morphological features can be altered by controlling the deposition parameters, like plasma power, substrate temperature, and oxygen partial pressure. C.C. Liao et al. [17] prepared nanocrystalline WO_3 thin films on solid substrates using spray and electroplating techniques and studied their

K. Hari Krishna · O.M. Hussain (✉)
Thin Film Laboratory, Department of Physics, Sri Venkateswara University, Tirupati 517 502, India
e-mail: hussainsvu@gmail.com

C.M. Julien
Institut des Nanoscience de Paris, UMR 7588, Unversite Pierre et Marie Curie, 140 Rue de Lourmel, 75015 Paris, France

electrochromic properties and observed 58.7% of optical modulation in 340–700 nm wavelength region. Thin films of WO_3 were deposited on glass substrates using pulsed DC magnetron sputtering by A. Subrahmanyam et al. [18]. They investigated the influence of oxygen sputter gas on electrochromic properties of WO_3 thin films and reported coloration efficiency of 141 cm^2/C for the films grown at higher oxygen partial pressures. M. Deepa et al. [19] investigated the electrochromic properties of spin coated nanostructured WO_3 thin films and observed 41.1 cm^2/C coloration efficiency at the wavelength of 550 nm. K.J. Lethy et al. [20] prepared WO_3 thin films by reactive pulsed laser deposition technique on glass substrates and studied the influence of substrate temperature on optoelectrochromic properties. Y. Suda et al. [21], A. Azens et al. [22] were deposited WO_3 thin films on ITO-coated flexible substrates using pulsed laser deposition and sputtering techniques, respectively, and studied their electrochromic and electrochemical properties to check their adaptability as active layers in electrochromic windows. In the current chromogenic technology, the deposition of metal oxide thin films on flexible substrates and their adaptability as an active layer in electrochromic windows is the current challenging and dynamic object for electrochromic community. These flexible substrates are unique in comparison to solid glass substrates, such as (1) they are flexible so that they can bend and stick to any curved shape objects with out altering their basic properties, (2) they are weightless, easy to carry, and can be fold. Hence the present investigation is aimed to prepare WO_3 thin films on ITO-coated flexible Kapton substrates using plasma-assisted activated reactive evaporation technique. The films were deposited at various deposition conditions and studied their structural, optical, and electrochromic properties. The influence of growth and microstructure on optoelectrochromic properties of the grown WO_3 thin films is investigated for their effective utilization as active layers in electrochromic (EC) windows.

2 Experimental details

The WO_3 thin films were deposited by using home-built activated reactive evaporation system [23]. A DC power supply with a current rating of 1 A at 2000 V was used as the power source. The deposition chamber was initially evacuated to a base pressure of 5×10^{-6} Torr and high-purity oxygen was allowed as the reacting gas and its flow was controlled by using Tylon mass controller. High density of plasma was created between the source and substrate by pumping the oxygen between the electrodes and by applying high DC voltage across the two electrodes. During the film deposition, the substrates are maintained in the temperature range 30–350°C.

The structural characteristics of the as-deposited WO_3 thin films were investigated using X-ray diffraction (XRD) technique (Siefert computerized X-ray diffractometer, model 3003 TT). Atomic force microscopy (AFM) (Digital Instrument: Dimension 3100 series) was used to study the surface morphology of the films in a simple contact mode of operation. The Raman spectroscopy measurements were performed at room temperature with a Jobin Yvon U1000 double monochromator using 514.5 nm line of argon (Spectra Physics) laser at a power level of 100 mW. The optical measurements were carried out by Hitachi U-3400 UV-VIS-NIR double beam spectrophotometer in the wavelength range of 300–1500 nm. The electrochromic coloration studies for tungsten trioxide thin films are performed by employing the dry lithiation method [24]. In this method, lithium niobate ($LiNbO_3$) powder was heat-treated at 840°C under high vacuum to give off lithium atoms for insertion in the exposed tungsten trioxide films. The quartz crystal monitor was used for the measurement of the film thickness during lithiation process to control and calibrated the thickness of the deposited $LiNbO_3$ film against the electrochemical insertion. The lithium atoms were exorcised from the lithium niobate powder during the heat treatment and intercalated into the tungsten trioxide thin films to give coloration for the films. Both coloration and marginal change in thickness of the tungsten trioxide films after lithium ion intercalation into the films confirms the diffusion of Li^+ ions into the films. This process has repeated at various time intervals and optimized the thickness of deposited Li layers for maximum coloration. In the present investigation 20-nm effective mass thickness of lithium layer is considered for maximum coloration, which corresponds to approximately 12.5 mC/cm^2 as verified from the electrochemical method.

3 Results and discussion

3.1 XPS studies

In the present investigation, the film depositions were carried out at an optimized discharge plasma power and oxygen partial pressures of 8 W and 1×10^{-3} Torr, respectively [25], and by varying the substrate temperatures (T_s) in the range 30–350°C. The X-ray photoelectron spectrum of the WO_3 films grown at $T_s = 250$°C demonstrated a characteristic doublet W 4f peaks (caused by spin-orbit splitting in tungsten and O (1s) core level) at core level binding energies of 36.1 and 38.2 eV corresponding to W $4f_{7/2}$ and W $4f_{5/2}$ peaks as shown in the Fig. 1. The peak respective positions of W 4f doublet peaks and their peak maxima separation value of 2.1 eV were in a good agreement with the powder data of WO_3 and these results enumerate that the tungsten in the deposited films exists in W^{6+} state [26].

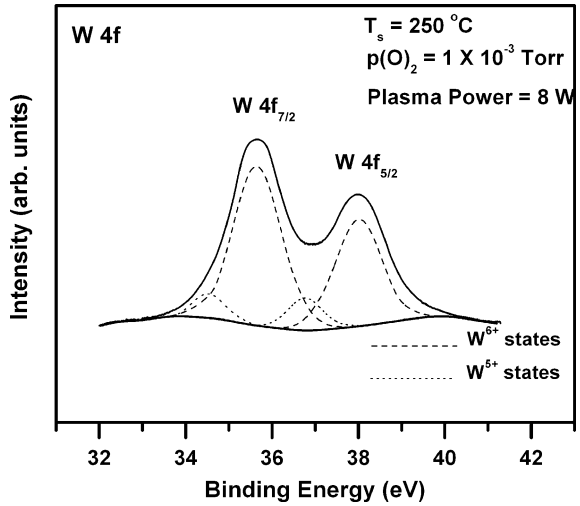

Fig. 1 The X-ray photoelectron spectrum of WO_3 thin film grown at $T_s = 250°C$, $p(O)_2 = 1 \times 10^{-3}$ Torr and plasma power = 8 W

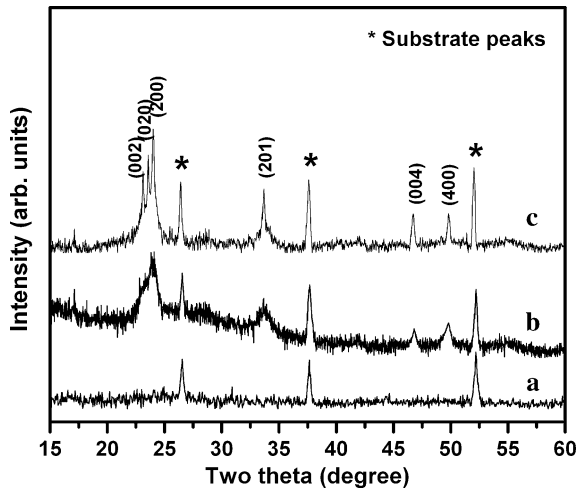

Fig. 2 The XRD patterns of WO_3 thin films grown at various substrate temperatures at (**a**) $T_s = 100°C$, (**b**) $T_s = 250°C$ and (**c**) $T_s = 350°C$

3.2 Structural studies

The XRD patterns of activated reactive evaporated WO_3 thin films deposited at various substrates temperatures are shown in the Fig. 2. For films grown at $T_s < 150°C$, the respective XRD patterns exhibited diffused and noncharacteristic features by revealing the X-ray amorphous nature of the films. The distinguished broad envelope is observed at around diffraction angle (2θ) of 23° for the films deposited at $T_s = 150°C$, which reveals the onset of crystallinity in the films and may be due to the presence of nanocrystallites in an amorphous matrix of WO_3 films. At the higher substrate temperatures, the envelope is noticed to be well-resolved and displayed three characteristic Bragg reflections at respective diffraction angles in the 2θ range 23–25°. For the films prepared at $T_s = 250°C$, the XRD pattern of the film demonstrated broad diffraction triplet peaks from (200), (020), and (002) reflections, in which (200) orientation is observed to be predominant. The crystallinity in the films and size of the crystallites are evaluated by considering the full width at half maximum (FWHM) value of (200) orientation. The Scherrer's formula is employed to estimate the size of the crystallites and found to be in the order of 65 nm for the films grown at $T_s = 250°C$. With the enhancement of substrate temperature ($T_s > 250°C$) the characteristic diffraction peaks are observed to be become sharper and respective XRD patterns of the films demonstrated two peaks (040) and (400) additionally at 46.2 and 49.5° along with characteristic peaks. The films grown at higher substrate temperature were found to be polycrystalline with monoclinic nature.

The growth of metal-oxide thin films on Kapton substrates may lead to the generation of stress components in the films. During the deposition of WO_3 thin films on Kapton substrates using plasma-assisted activated reactive evaporation technique, the evaporated species reach the surface of substrate with greater kinetic energy by passing through the high-density plasma. This process favors for the formation of a greater number of crystallite centers rather than coalescence of islands. The rate of adatom mobility on surface of substrates may be relatively smaller at lower substrate temperature. Hence vertical growth of grains perpendicular to the substrate surface is observed and may be responsible for the existence of more stress and strain components in the films. The tensile and compressive stresses are generated during deposition of the films. The tensile stresses may be explained by the grain–boundary relaxation model [27] and the strain is generated from the interatomic attractive forces along the constrained grains. Whereas the compressive stresses arise because of the compressive strain in the crystal grains. The estimated stress components are observed to be decreased with the increase of substrate temperature. The evaluated stress component value for the nanocrystalline WO_3 films grown at $T_s = 250°C$ are found to be about 1.56×10^9 Pa, which are observed to be slightly higher than that of the films grown on glass substrates.

3.3 Surface morphology

The surface morphology of the deposited WO_3 thin films has been examined as a function of substrate temperature by atomic force microscopy (AFM). The as-deposited WO_3 thin films grown at $T_s < 150°C$ are demonstrated fairly smooth surfaces with minute graininess by indicating amorphous nature of the films (Fig. 3a). Despite this mild grainy appearance, the films are quite reflective representing the optical flatness of the film surface. The surface morphological features are noticed to be predominant at $T_s > 150°C$ and

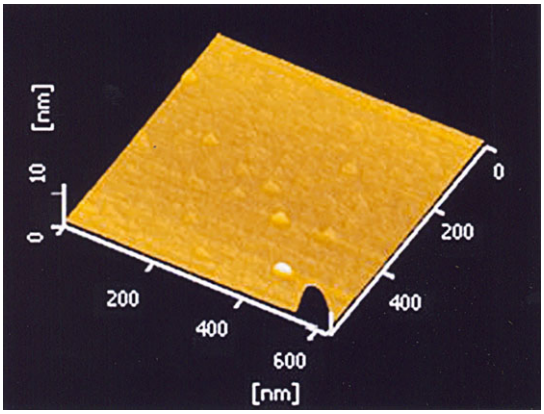

a

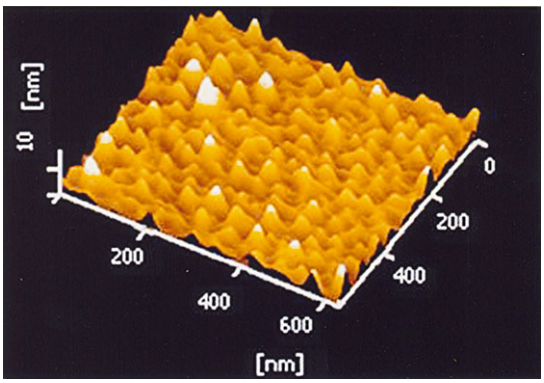

b

Fig. 3 The atomic force micrographs of WO_3 thin films grown at various substrate temperatures (**a**) $T_s = 100°C$ and (**b**) $T_s = 250°C$

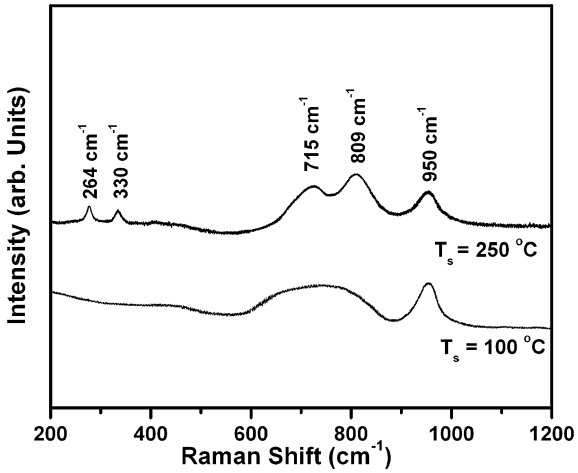

Fig. 4 The Raman spectra of WO_3 thin films grown onto flexible ITO-coated Kapton substrates as a function of substrate temperature in the range 100–350°C

respective changes are associated to the size and shape of the grains. The WO_3 films prepared at $T_s = 250°C$ exhibited surface morphology composed of vertically elongated cone shape and provided with sharp-headed nanograins of size in the order of 70 nm. These nanosized grains are observed to be individual, bound tightly together with high density of interfaces, grain boundaries provided with good intergranular contacts and internal volume as shown in the Fig. 3. This type of micro porous, nano particulate surface morphology of WO_3 films is the most beneficial characteristic property for efficient ion insertion–extraction process in an electrochromic system. The other prominent characteristic features in the present study are the changes in surface morphology of the ARE WO_3 films as a function of substrate temperature. At a higher substrate temperature, the mobility of adatoms enhances on the surface of the substrates, which leads to overcome the potential energy of the nucleation sites on the substrate with net increase in the diffusion distance. In addition to this, the collision process initiates the nucleation and favors for the island formation in order to grow continuous film with larger grains. The estimated root mean square surface roughness of the films is also varied as a function of substrate temperature and found to be increased from 3 to 11 nm with the increase of substrate temperature from 30 up to 350°C, respectively. In the present study, the growth of crystallites were observed to be vertical due to less rate of adatom mobility on surface of the substrates maintained at reasonable substrate temperature. Where as the films grown at identical conditions on ITO-coated glass substrates, due to the high kinetic energy of the crystallites and adatom mobility, the coalescence between the crystallites occur predominantly and the grain growth is observed to be parallel to the substrate surface.

3.4 Raman studies

Figure 4 illustrates the Raman spectroscopic measurements in the wavenumber range 200–1200 cm^{-1} for WO_3 thin films deposited at various substrate temperatures in the range 30–350°C. For the films prepared at $T_s < 150°C$, the Raman spectrum of the films demonstrated noncharacteristic broad band in the wave number range 600–900 cm^{-1} and its center of gravity is observed to be located at around 770 cm^{-1}. A strong and relatively high-intensity Raman peak is observed at the wave number of 950 cm^{-1} by indicating the amorphous nature of the films. This narrow Raman band present at the wave number of 950 cm^{-1} corresponds to the W^{6+}=O stretching modes of terminal oxygen atoms possibly on the surfaces of the cluster and micro void structure in the films [28]. The center of gravity of the broad band corresponds to W–O stretching modes is noticed to be shifted towards higher wave number side. This broad band is observed to be well resolved with the enhancement of substrate temperature higher than 150°C. In addition to this, the intensity of the strong intense Raman peak (RS) lies

at wave number of 950 cm^{-1} (W=O) is noticed to be decreased and become relatively broader with the increase of substrate temperature. This result enumerates the augmentation of size of the crystallites and suggests the commencement on set of crystallinity in the grown films. The center of gravity of the broad band present in the wave number range (600–900 cm^{-1}) is shifted to 798 cm^{-1} and exhibited better resolved characteristic Raman peaks at the wave numbers of 715 and 809 cm^{-1} with the enhancement of substrate temperature to the higher value of 250°C. The assigned Raman peaks are observed to be broader and the respective full width at half maximum (FWHM) values of the peaks are relatively higher by revealing the presence of nanosized crystallites in the films grown at the substrate temperature of 250°C. The intensity of the characteristic Raman peaks increased and two additional Raman peaks are observed with the increase of substrate temperature higher than 300°C at 264 and 330 cm^{-1}, which attributed to the bending vibration of δ(W–O–W) bonds. For the tungsten trioxide films deposited at higher substrate temperature of 350°C, the respective Raman spectrum demonstrated sharper and well-resolved characteristic Raman peaks at the wave numbers of 715 and 809 cm^{-1}, which are attributed to the monoclinic structure. The respective monoclinic phase belongs to the $P2_1/n$ ($C^5 2h$) space group, which has 96 modes of which 48 are Raman active. The estimated intensities ratio of (W=O/W–O) is observed to be decreased from 1.6 to 0.65 with the increase of substrate temperature from 150 to 350°C revealing the increase in crystallinity in the films. Therefore from the above extensive analyses the WO_3 films deposited at $T_s < 150$°C were amorphous and films grown at $T_s > 300$°C were found to be polycrystalline in nature. The films grown at $T_s = 250$°C were nanocrystalline composed of nanosized grains of size about 70 nm.

3.5 Optical properties

The optical transmittance spectra of WO_3 thin films grown at various substrate temperatures are recorded in the wavelength range 300–1500 nm and are shown in the Fig. 5. The sharp fall in the optical transmittance spectra observed in the region of 300–400 nm is due to the fundamental absorption edge. The oscillations in the transmission spectra are caused by optical interference arising due to difference of refractive index of thin films with substrate and the interference of multiple reflections originated from film and substrate surfaces. From the obtained optical transmittance spectra, both amorphous and polycrystalline WO_3 films demonstrated dominant interference pattern in visible-near-infrared region. But the nanocrystalline films do not exhibit any strong oscillations in throughout transmittance spectrum; this optical behavior may be due to the highly porous and grainy surface of the films. The amorphous tungsten trioxide films

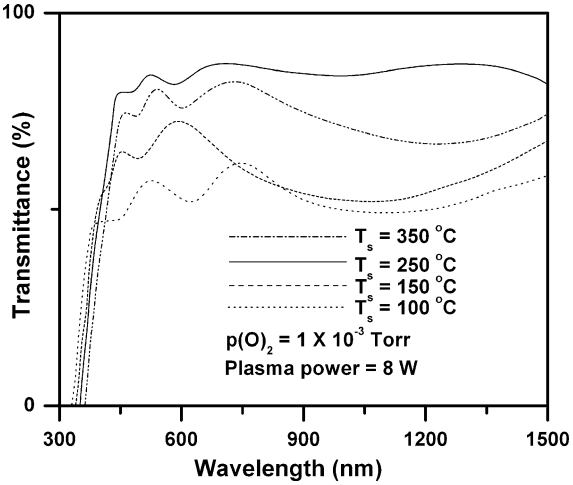

Fig. 5 The variation of optical transmittance of activated reactively evaporated WO_3 thin films grown at various substrate temperatures in the range 100–350°C

($T_s < 150$°C) are exhibited relatively lower optical transmittance in the order of 60% in the visible region. Significantly, the fundamental absorption edge demonstrated positive shift in the wavelength (i.e., redshift) with the increase of substrate temperature (>150°C, i.e., with the increase of grain size), which indicates a shift in the optical band gap towards lower energy. The increase in optical transmittance of the films is observed with the increase of substrate temperature and the nanocrystalline WO_3 films grown at $T_s = 250$°C demonstrated higher optical transmittance of 85% in the most of the spectral region studied leading to a very neutral appearance. Further, the decrease in optical transmittance is noticed for the films grown at $T_s > 300$°C and the polycrystalline tungsten trioxide thin films deposited at $T_s = 350$°C exhibited lower optical transmittance 70% in the visible region in comparison to the nanocrystalline films. The appreciable decrease in optical transmittance observed for tungsten trioxide thin films grown at $T_s > 300$°C may attribute to the transition from nanocrystalline state to polycrystalline state as evidenced from XRD and AFM measurements.

The optical absorption coefficient (α) of the activated reactive evaporated WO_3 films is evaluated for all the films. The optical band gap was evaluated by extrapolating the linear region of the plot $(\alpha h\nu)^{1/2}$ versus $h\nu$ to zero absorption and the variation of estimated optical band gap values of WO_3 films as a function substrate temperature is shown in the Fig. 6. The amorphous WO_3 films prepared at room temperature were exhibited higher optical band gap value of 3.42 eV, this may be due to the result of quantum size effects due to the small WO_3 cluster size. The considerable change in optical band gap values is not observed with the increase of substrate temperature from 30 to 150°C, as shown in Fig. 6. Further slight decrease in optical band gap

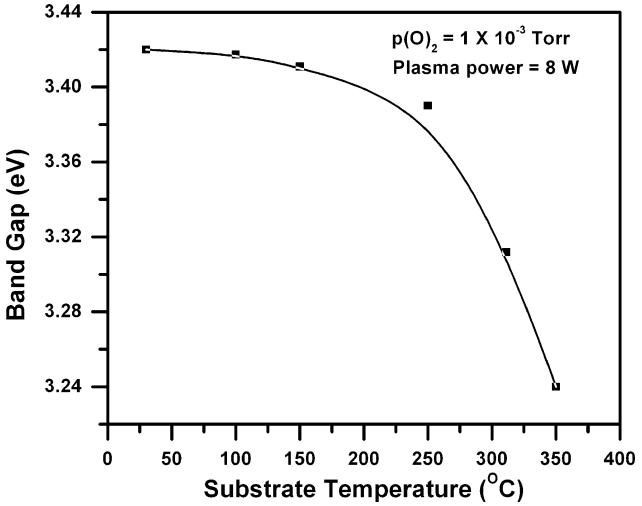

Fig. 6 The variation of optical band gap as a function substrate temperature

value is observed with the increase of substrate temperature (>150°C) and the nanocrystalline WO_3 films with grain size of 70 nm prepared at substrate temperature of 250°C exhibited an optical band gap value of 3.39 eV. But a monotonic drop in optical band gap values is observed with the increase of substrate temperature (>300°C) and size of the grains in the films. The polycrystalline WO_3 films with maximum grain size of 165 nm prepared at a substrate temperature of 350°C exhibited a relatively lower optical band value of 3.24 eV. The considerable blueshift in the absorption edge is observed for the amorphous WO_3 films, this may be due to existence very small particles, grain boundaries and imperfections, which lead to larger free carrier concentrations and existence of potential barriers. The electric fields arising from these factors result in a higher optical band gap value of the amorphous tungsten trioxide films, grown at lower substrate temperatures (<150°C). In addition to this, the band gap is sensitive function of W–O bond length. Therefore, in amorphous films the structural relaxation resulting in an increase of W–W distance and changes in W–O splitting. Consequently, the structural distortion in WO_6 octahedra can lead to the displacement of W ion from the center of the octahedra. This off-centering results in lowering of the valence band and raising the conduction band which leads to demonstrate higher optical band gap value for amorphous tungsten trioxide films. The monotonic drop in optical band gap value with the increase of substrate temperature higher than 300°C indicates the crystallization (i.e., transition from nanocrystalline to polycrystalline state as evidenced by XRD measurements and an increase in grain size), which causes narrowing of the band gap. In addition, there may be a contribution from internal stress developed in the polycrystalline film and effective decrease in the imperfections at grain–boundary regions. The AFM measurements indicated that the increase in grain size is associated with a random distribution of the grains on the film surface. The random distribution of the grains makes the film surface rough and the results in the increased light scattering losses at the interface. This accounts for the observed decrease in the transmittance with increasing substrate temperature (>300°C). These results enumerate the influence of grain size on optical properties of WO_3 films [29].

The effect of substrate temperature on the refractive index was investigated by means of spectroscopic ellipsometry. The estimated refractive index values for the films at a wavelength of 550 nm are observed to be increased exponentially with the increase of substrate temperature (i.e., increase of grain size). The evaluated refractive index values were found to be lower for amorphous films grown at $T_s = 30$°C and observed to increase with the enhancement of substrate temperature. For the nanocrystalline WO_3 films with grain size of 70 nm and RMS surface roughness of 8 nm, the estimated refractive index is noticed to be 1.92. The polycrystalline WO_3 films prepared at a substrate temperature of 350°C were showed to have higher refractive index value of 1.99. It is noteworthy that the electrochromic performance of the deposited WO_3 films is significantly influenced by the relative density and porosity of the films, which in turn depends upon the refractive index of the films. The relative density of thin-oxide films depends strongly on the film deposition parameters, which can tailor the relative packing density value of the films. The relative density of the films is calculated using Lorentz–Lorentz relation [30]. The estimated relative density of the films increased exponentially with the increase of substrate temperature. The as-deposited amorphous tungsten trioxide films prepared at room temperature demonstrated lower packing density value of 0.63 and the polycrystalline films prepared at a substrate temperature of 350°C demonstrated higher relative packing density value of 0.78, which indicates the densification of films by the impact of energetic particles on the growing film surface maintained at higher substrate temperatures. The porosity in the grown films is calculated from estimated refractive index values using first-order rule of mixtures, according to the following equation [31]:

$$(1 - X)n_{\mathrm{TD}} + Xn_{\mathrm{air}} = n_{\mathrm{means}} \quad (1)$$

where 'X' is porosity, n_{TD} is the refractive index of the film material; n_{means} is refractive index of the grown WO_3 thin film, and n_{air} refractive of air, which is taken as one. The estimated porosity values using above expression are observed to be decrease with the enhancement of substrate temperature. The estimated porosity values of the WO_3 films deposited at a substrate temperature of 250°C is observed to be 0.46.

3.6 Electrochromic properties

Figure 7 shows the dynamic modulation of optical transmittance in virgin and colored states in the wavelength range 300–1500 nm, for WO_3 films deposited at various substrate temperatures in the range 30–350°C. From the obtained results, apparently the activated reactively evaporated WO_3 films are demonstrating higher optical modulation in the visible region. In the present investigation, the optical modulation values of the grown films are evaluated at the wavelength of 550 nm. The variation coloration efficiency with the substrate temperature is shown in the Fig. 8. The amorphous WO_3 thin films prepared at a substrate temperature of 150°C are demonstrated a reasonable optical modulation of 39% in the visible region. But the WO_3 films prepared at higher substrate temperatures, i.e., the polycrystalline WO_3 films grown at 350°C exhibited comparatively lower optical modulation of 32%. The nanocrystalline tungsten trioxide thin films deposited at substrate temperature of 250°C are observed to exhibit a higher optical modulation of 66% at the wavelength of 550 nm.

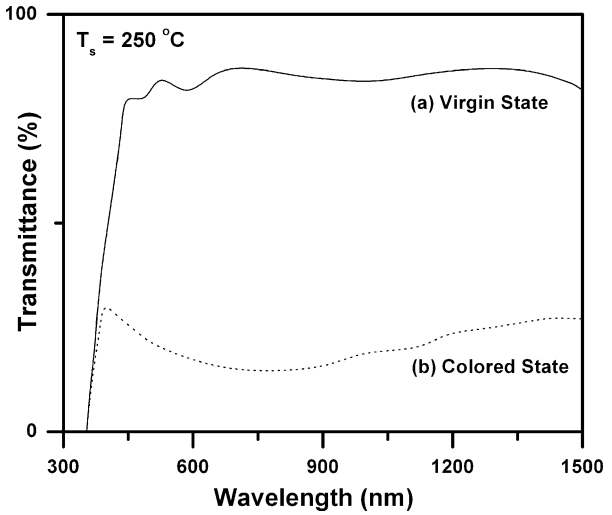

Fig. 7 The modulation of optical transmittance in nanocrystalline WO_3 thin film both in virgin and colored states

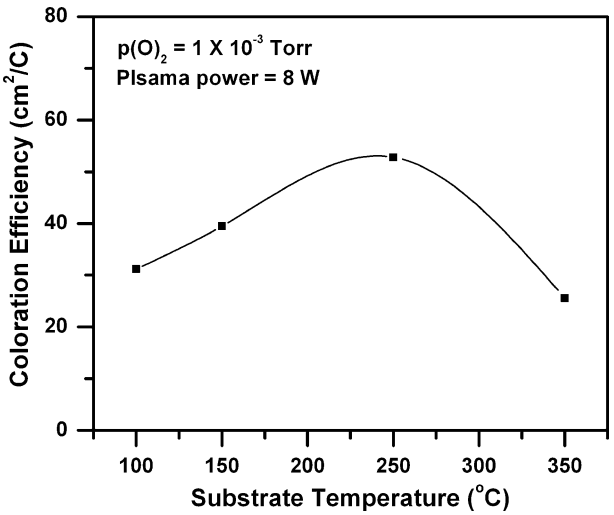

Fig. 8 The variation coloration efficiency of the WO_3 films as a function of substrate temperature

Generally, in simple transition metal oxide thin films with fine grainy surfaces, the optical modulation occurs due to *absorption modulation* caused by the development of an absorption band. In case of crystalline films, predominantly the *reflection modulation* is the responsible for lower optical modulation in the visible region. The electrochromic process in amorphous and nanocrystalline tungsten trioxide films can be attributed by adapting the concept of small polaron formation [32]. "The quasi particle composed of a self-trapped electronic carrier taken together with the pattern of atomic displacements, is known as polaron". A small polaron is formed in a covalent system in which only a short-range electron–lattice interactions occur. The displacing atoms or ions in material from their carrier-free equilibrium position produce a potential well that will bind a charge carrier by self-trapping. Resultantly all these potential wells combined and a polaron band is formed below the conduction band. The inserted free charge carriers were trapped by these potential wells and act as charges bound to defects or color centers. With the absorption of radiation, these self-trapped carriers could be carried out of the potential well and change the optical properties of the films. Therefore, the inserted electrons are located in W^{5+} sites and polarize their surrounding lattice to form small polarons. When the absorption of a photon of appropriate energy occurs by the self-trapped carrier (electron), it can be free from the potential well which self-traps the electrons. As a result, the electrons excite from the lower energy states (W^{5+}) to neighboring higher energy states (W^{6+}), this process is responsible for optical absorption in colored state. This process can be express as follows:

$$h\nu + W^{5+}(A) + W^{6+}(B) \rightarrow W^{6+}(A) + W^{5+}(B) \tag{2}$$

One of the most important criteria for selecting an electrochromic material is its coloration efficiency (CE), which is defined as the change in optical density (OD) per unit inserted charge (Q).

$$\mathrm{CE} = \frac{\Delta(\mathrm{OD})}{\Delta Q} = \frac{\Delta \log(T_b/T_c)}{\Delta Q} \tag{3}$$

High coloration efficiency can provide a large optical modulation with small charge insertion or extraction and is a crucial parameter for practical electrochromic devices because long-term cycling stability may be enhanced by using a lower charge or extraction rate. Using (3), the coloration efficiencies were evaluated for all type of films. The variation estimated coloration efficiency values as a function of

substrate temperature is shown in the Fig. 8. The amorphous WO_3 films ($T_s < 150$°C) exhibited coloration efficiency of 31.2 cm^2/C in the visible region and noticed to be decreased in the near-infrared region. The polycrystalline WO_3 films ($T_s = 350$°C) with maximum grain size of 148 nm demonstrated relatively lower CE values both in visible and infrared regions and found to be 25.6 cm^2/C in the visible region at the wavelength of 550 nm. But the nanocrystalline tungsten trioxide films ($T_s = 250$°C) composed of nanosized grains of size 70 nm demonstrated higher CE of 52.8 cm^2/C (at the wavelength of 550 nm) in the visible region and lesser CE values in infrared region. This can be explained as follows: the nanocrystalline films are characterized by their crystallite sizes in the nanometric range, they posses a large internal volume (or porous) while maintaining a fairly high intercrystallite contact essential for electrochromic conductivity in the films. The large internal volume raises the electrochromic kinetics and percolating the amount of ions and electrons, which endorse the coloration efficiency. In addition, the nanopores in nanocrystalline WO_3 film are easier to absorb water in the pores than the amorphous films. Therefore the absorbed water in the nanopores helps the diffusion of ions and electrons in the electrochromic modulation. The existed nanoscale pores and grains are most beneficial for fast lithium-ion insertion and extraction during intercalation studies. The initial high transmission of these films also contributes to the electrochromic modulation. Such nanocrystalline films generally have an elevated level of normal state of transmittance and are shown to exhibit a superior degree of electrochromic optical modulation and coloration efficiency in comparison to conventional amorphous and polycrystalline films.

4 Conclusions

Plasma-assisted activated reactive evaporation technique has been employed for the growth of WO_3 thin films on ITO-coated flexible Kapton substrates. The microstructural and optoelectrochromic properties of the grown WO_3 thin films are observed to be strongly influenced by the deposition temperature. The films grown at plasma power of 8 W in an oxygen partial pressure of 1×10^{-3} Torr and at a substrate temperature of 250°C were found to be nanocrystalline in nature. The X-ray diffraction spectra of WO_3 films grown at $T_s < 150$°C exhibited a diffused and not characteristic feature by indicating the amorphous nature of the films and found to be polycrystalline at higher substrate temperatures (>250°C). The center of gravity of the broad band in the wave number range 600–900 cm^{-1} corresponds to W–O stretching modes is noticed to be shifted towards higher wave number side with the enhancement of substrate temperature (>150°C). The estimated intensities ratio of (W=O/W–O) is observed to be decreased from 1.6 to 0.65 with the increase of substrate temperature from 150 to 350°C revealing the enhancement of in crystallinity in the films. The nanocrystalline WO_3 films exhibited microporous, nanoparticulate surface morphology, which is the most beneficial characteristic property for efficient ion insertion–extraction process in an electrochromic system. The optical transmittance of films increased with the augmentation of substrate temperature up to 250°C and further declined with the increase of substrate temperature. The nanocrystalline films composed of vertically elongated cone shape and provided with sharp-headed nanograins of size in the order of 70 nm were demonstrated higher optical transmittance of 85% in the visible range. The nanocrystalline WO_3 films prepared at $T_s = 250$°C exhibited an optical modulation of 66% with coloration efficiency of 52.8 cm^2/C at the wavelength of 550 nm. These nanocrystalline WO_3 films can be adapted as active layers in electrochromic windows.

References

1. A. Rouger, F. Portemer, A. Quede, M.E. Marssi, Appl. Surf. Sci. **153**, 1 (1999)
2. C.G. Granqvist, Sol. Energy Mater. Sol. Cells **60**, 201 (2000)
3. C.G. Granqvist, Solid State Ion. **53–56**, 479 (1992)
4. S.A. Agnihotry, R. Ramachandran, S. Chandra, Sol. Energy Mater. Sol. Cells **36**, 289 (1995)
5. A. Azens, C.G. Granqvist, J. Appl. Electrochem. **7**, 64 (2003)
6. P.S. Patil, P.R. Patil, S.S. Kamble, S.H. Pawer, Sol. Energy Mater. Sol. Cells **60**, 143 (2000)
7. H. Kaneko, F. Nagao, K. Miyake, J. Appl. Phys. **63**, 510 (1988)
8. H. Qiu, Y.F. Lu, Z.H. Mai, J. Appl. Phys. **91**, 440 (2002)
9. A. Bessiere, C. Marcel, M. Morcrette, J.-M. Tarascon, V. Lucas, B. Viana, N. Baffier, J. Appl. Phys. **91**, 1589 (2002)
10. S.K. Deb, Sol. Energy Mater. Sol. Cells **92**, 245 (2008)
11. O.M. Hussain, A.S. Swapna Smitha, J. John, R. Pinto, Appl. Phys. A **81**, 1291 (2005)
12. L.J. LeGore, R.J. Lad, S.C. Moulzolf, J.F. Vetelino, Thin Solid Films **406**, 79 (2002)
13. G.G. Belmonte, V.S. Vikhrenko, J.G. Canadas, J. Bisquert, Solid State Ion. **170**, 123 (2004)
14. S. Penner, X. Liu, B. Klotzer, F. Klauser, B. Jenewein, E. Bertel, Thin Solid Films **516** (2008)
15. Y. Djaoued, S. Priya, S. Balaji, J. Non-Cryst. Solids **354**, 673 (2008)
16. E. Ozkan, F.Z. Tepehan, Sol. Energy Mater. Sol. Cells **68**, 265 (2001)
17. C.C. Liao, F.R. Chen, J.J. Kai: Sol. Energy Mater. Sol. Cells **91**, 1282 (2007)
18. A. Subrahmanyam, A. Karuppasamy, Sol. Energy Mater. Sol. Cells **91**, 266 (2007)
19. M. Deepa, T.K. Saxena, D.P. Singh, K.N. Sood, Electrochim. Acta **51**, 1974 (2006)
20. K.J. Lethy, D. Beena, R. Vinod Kumar, V.P. Mahadevan Pillai, Appl. Surf. Sci. **254**, 2369 (2008)
21. Y. Suda, H. Kawasaki, T. Ohshima, Y. Yagtuu, Thin Solid Films **516**, 4397 (2008)
22. A. Azens, E. Avendano, J. Backholm, L. Berggren, G. Gustavsson, R. Karmhag, G.A. Niklasson, A. Roos, C.G. Granqvist, Mater. Sci. Eng. B **119**, 214 (2005)

23. O.M. Hussain, K.S. Rao, Mater. Chem. Phys. **80**, 638 (2003)
24. P.V. Ashrit, Thin Solid Films **285**, 81 (2001)
25. K. Hari Krishna, O.M. Hussain, C. Guillen, Optoelectron. Adv. Mater.—Rapid Commun **2**, 242 (2008)
26. L. Lozzi, L. Ottaviano, M. Passacantando, Thin Solid Films **391**, 224 (2001)
27. R.W. Hoffman, Thin Solid Films **34**, 185 (1976)
28. G. Fang, Z. Liu, K.L. Yao, J. Phys. D. Appl. Phys. **34**, 2260 (2001)
29. C.V. Ramana, R.J. Smith, O.M. Hussain, Phys. Status Solidi **199**, R4 (2003)
30. E. Washizu, A. Yamamoto, Y. Abe, M. Kawamura, K. Sasaki, Solid State Ion. **165**, 175 (2003)
31. H. Xie, J. Wei, X. Zhang, J. Phys., Conf. Ser. **28**, 95 (2006)
32. V. Wittner, O.F. Schirmer, P. Schotter, Solid State Commun. **25**, 977 (1978)